CAD Applying the Finite-Element Method for Dielectric-Resonator Filters

Dominique Baillargeat, Serge Verdeyme, Michel Aubourg, and Pierre Guillon, *Senior Member, IEEE*

***Abstract*— The progress of numerical techniques now permit us to analyze rigorously complex devices such as dual-mode cavity multipole filters or planar passive elements for coplanar monolithic microwave integrated circuits (MMIC's). In this paper, we describe a rigorous design of dielectric resonator (DR) filters applying the finite-element method (FEM). We first present a dual mode coupling technique which replaces classical DR's, coupling, and tuning screws, which are commonly used in dual-mode filters, by slotted DR's. Next, a new theoretical analysis based on the contribution to the dual-mode filter response of the first DR hybrid mode and of higher order modes is described. This analysis can be applied to any type of microwave dual-mode filter. It allows us to define a procedure which explains the presence and controls the position of the two transmission zeros in the filter responses. In this paper, this procedure has been applied to improve filtering performances of a dual-mode DR filter. Finally, a synthesis method is developed to rigorously design for the first time, a four- and an eight-pole slotted DR elliptic filters. The experimental results were obtained with no tuning and the theoretical ones show good agreement.**

***Index Terms*— CAD, dielectric resonator, filter, finite-element method, rigorous design.**

I. Introduction

TODAY, many types of passive microwave filters are developed. They can be divided into two principal categories. The planar ones can be composed of microstrip, stripline, or coplanar resonators. They are used in a large frequency domain (100 MHz–30 GHz) to realize generally large band response filters, due to their low unloaded quality (Q_u) factor. For the last few years, their losses can be compensated by active devices or superconducting technology. For special applications, their small dimensions and their excellent compatibility with an electronic surrounding are of great interest. The second category, the voluminous filters, is composed of metallic cavities, waveguides, or dielectric resonators (DR's). These filters present a high unloaded Q_u factor and a high-temperature stability which permit us to achieve very narrow bandwidth in a large frequency domain (900 MHz–100 GHz). They are also required for power applications, but their large dimensions and a delicate compatibility with an electronic environment can be a disadvantage for some system development.

In most cases, during the first conception of planar or voluminous complex filters, some differences appear between theoretical and experimental results which impose experimental tuning to satisfy filtering objectives. To eliminate this tuning, numerical techniques have been developed and permit us to now rigorously analyze complex microwave devices. Different authors [1]–[4] have recently published the whole rigorous analysis of dual-mode cavity multipole filters. Numerical modeling of planar passive elements, such as coplanar ones for monolithic microwave integrated circuits (MMIC's) [5], have also been presented.

We project here to develop rigorous design of DR filters. Indeed, these filters and, in particular, dual-mode filters are widely used in telecommunication systems because they offer better performances, smaller size, and less weight than classical fundamental TE- or TM-mode filters [6], [7]. Moreover, this configuration may simplify the achievement of elliptic responses to increase the filter rejection slope. It is well known that a cylindrical DR shielded in a cylindrical metallic cavity presents on the first hybrid mode $\mathrm{HEM}_{11\delta}$ two orthogonal polarizations at the same frequency. Generally, the coupling between the two polarizations is produced by adding a metallic screw or any discontinuity in the DR environment, located in 45° angle with respect to each excitation probe direction. The filter response can be adjusted by changing the penetration in the DR enclosure of the coupling and tuning screws, but these systems are not rigorously taken into account by actual theoretical methods. Thus, each experimental realization requires long and delicate tuning, which may increase the cost of dual-mode DR filter production. Our objective is to develop a rigorous analysis to eliminate these tunings.

This paper concerns a dual mode coupling technique which replaces classical dual-mode DR structures (e.g., classical DR's, metallic screws) by slotted DR's excited on the first hybrid mode [8]. The device under consideration is described in Fig. 1. Using the three-dimensional (3-D) finite-element method (FEM), we first present the notch-1 effect on the coupling between the two resonant dual modes. This FEM rigorous analysis permits us to explain the presence or the absence of two transmission zeros in the filter response. Then, a procedure developed to predict the frequency position of these transmission zeros allows us to obtain the symmetrical dual-mode filter responses. Finally, the out-of-band isolation for an asymmetrical and a symmetrical response is presented.

The second part of this paper presents the application of the slotted DR coupling technique. Thus, a theoretical method using the 3-D FEM is developed to analyze dual-mode filter responses. Two elliptic filters with four and eight poles are rigorously designed. For the first one, dielectric and metallic losses are taken into account. Before the experimental realizations, the notches and coupling iris manufacturing tolerances have been defined applying a sensitivity analysis.

Manuscript received October 17, 1995; revised October 9, 1997.

The authors are with IRCOM–UMR, Université de Limoges, 87060 Limoges, France.

Publisher Item Identifier S 0018-9480(98)00634-6.

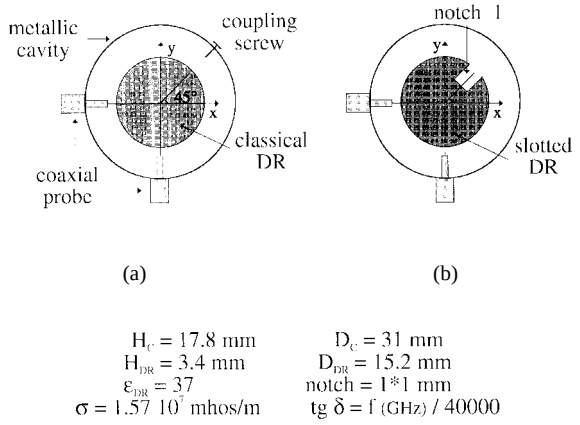

Fig. 1. Classical and slotted cylindrical DR.

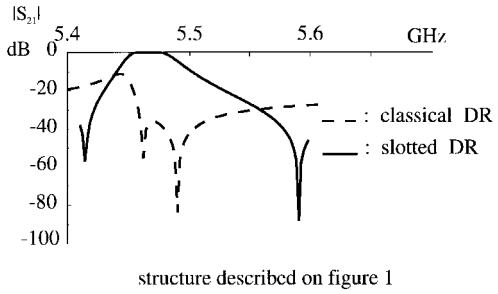

Fig. 2. Insertion–loss responses of a classical and a slotted DR.

Finally, the two elliptic filters have been built and tested without tuning. Comparisons between theoretical and experimental results show encouraging agreement.

II. Numerical Analysis

The theoretical analysis is performed applying the free or forced oscillations 3-D FEM between the access ports of the device. The FEM is well known to be useful for solving Maxwell's equations. This method has already been explained in several papers [9], [10] and our purpose is not to describe it here. The mathematical formulation we solve is identical to the commercial simulator HFSS.[1] We can notice that the device under consideration is meshed with triangles [two-dimensional (2-D)] or tetrahedrons (3-D). To solve the Maxwell's equations on each node of the mesh, we apply a vectorial E-formulation using mixed finite elements of Nedelec with second-order polynomials. Indeed, this formalism permits us to avoid spurious responses [9], [11]. Moreover, using our electromagnetic software, we can analyze complex voluminous or planar devices. The inner materials must be homogeneous and linear, but can be anisotropic and possess dielectric or metallic losses. The studied structure is generally closed by perfect magnetic and electrical conditions or excited by transmission lines or waveguides. Absorbing conditions are introduced to analyze open devices. For the forced oscillations problem imposing the frequency, we obtain the scattering matrix parameters between the physic access ports. For the free oscillations one, these planes may also be short circuited and the analysis gives the resonant frequency, field repartition of each eigenmode, and their unloaded Q_u factor.

[1] HFSS, Hewlett-Packard Co., Santa Rosa, CA, 1994.

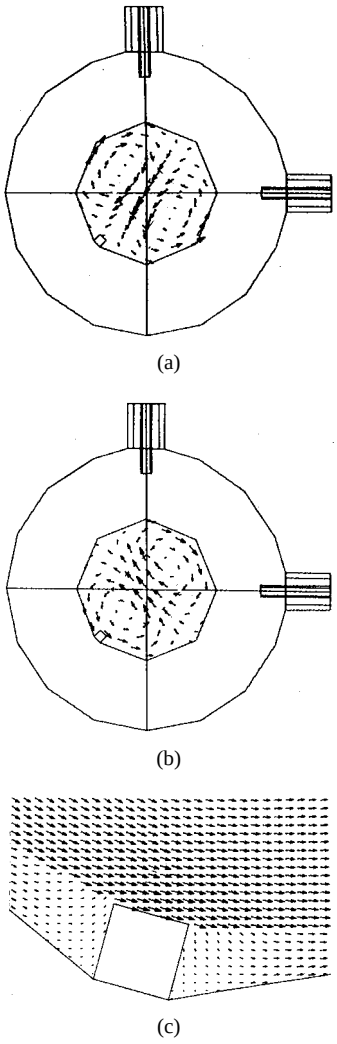

Fig. 3. Electromagnetic-field lines.

III. Slotted Dielectric Resonator

Using the forced oscillations' 3-D FEM, we consider a classical or a slotted cylindrical DR shielded in a metallic cavity, as shown in Fig. 1. The S_{21} modulus parameter computed in the access ports, proves that the microwave power is only transmitted between these ports by the slotted DR. Thus, we obtain a bandpass response for this device (see Fig. 2), and it seems that the classical coupling screw can be replaced by notch 1.

A second study using the free oscillations 3-D FEM allows us to define for a slotted DR the two orthogonal hybrid mode resonant frequencies f_1 and f_2 for given notch-1 dimensions. The two polarization electromagnetic-field lines obtained by free-running analysis are shown in Fig. 3. It appears that the polarization planes are defined by the notch location. For one of the modes, the field configuration [Fig. 3(a)] is not modified by the presence of the notch and its frequency f_1 is constant as a function of the notch dimensions. The second frequency f_2 depends on the notch dimensions. Indeed this notch disturbs the mode field lines [see Fig. 3(b) and (c)]

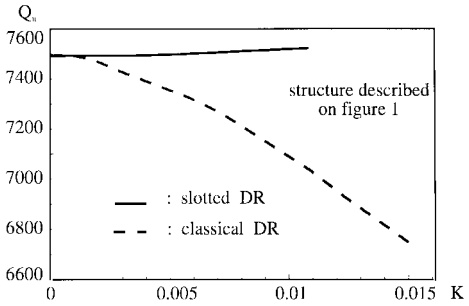

Fig. 4. Unloaded Q_u factor of a classical and a slotted DR as a function of K.

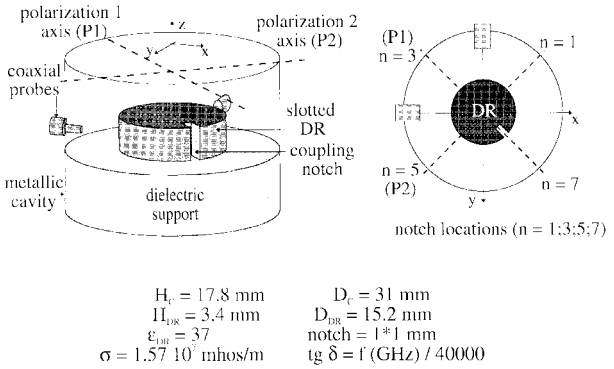

Fig. 5. Dual-mode slotted-DR filter.

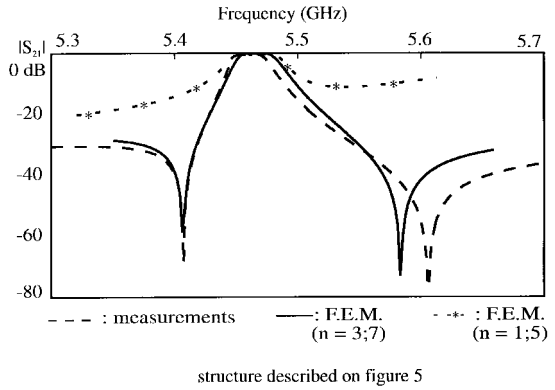

Fig. 6. Computed and experimental insertion–loss response of the two-pole filter.

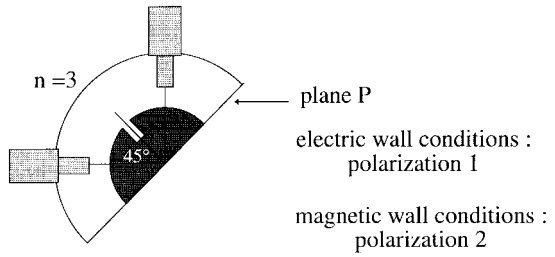

Fig. 7. Electric- or magnetic-wall conditions. Polarization 1 or 2.

imposing quasi-magnetic-wall conditions on its faces. Thus, this notch produces a frequency shift between the two resonant frequencies f_1 and f_2. We can then consider the filter response as the sum of each polarization contribution.

Fig. 4 presents the unloaded Q_u factor computed as a function of the coupling coefficient K [12] between the two polarizations for a classical DR with a coupling screw [see Fig. 1(a)] and for a slotted one [see Fig. 1(b)]:

$$K = \frac{f_1^2 - f_2^2}{f_1^2 + f_2^2}. \tag{1}$$

For coupling values higher than five 10^{-3}, the distance between the screw and the DR is inferior to 1.5 mm. Moreover, to increase this coupling, this distance must decrease. Then, as is shown in [13], for these conditions, the metallic losses of the device increase and the Q_u decreases. Using the slotted DR, the Q_u factor seems to increase with K due to the decrease of dielectric material. However, these last Q_u level variations are not significant for filtering applications, so we can say that a slotted DR advantage compared to the classical DR is to preserve the Q_u quasi-constant for these filtering applications.

We now analyze the device described in Fig. 5 where the coupling notch can be placed in the different ports 1, 3, 5, and 7. Using the forced oscillations' 3-D FEM between the access planes, the reflection and the transmission responses of the device are computed, as shown in Fig. 6. The same responses without transmission zeros are obtained for the locations $n = 1; 5$. The locations $n = 3; 7$ permit us to generate high rejection slopes and then better filtering performances. This phenomena, verified by measurements, has been observed for a classical DR with a coupling screw in these different planes [12], [14]. It has been allocated to a direct coupling between the probes through an induced current on the metallic screw for locations 3 and 7. However, with the slotted DR, there is no metallic part, so the FEM was used to find another explanation. We have considered the device defined in Fig. 7. By imposing, respectively, electric- and magnetic-wall conditions on plane P, we can evaluate each polarization contribution on the device response. For each case, we present in Figs. 8 and 9 the insertion–loss characteristic and phase parameters. In Fig. 8, the first transmission peak at approximately 5.45 and 5.48 GHz in the insertion–loss curves are the DR $\mathrm{HEM}_{11\delta}$-mode resonance for each polarization. The second peak, at approximately 6.16 GHz, are the resonance of the first higher order mode. This higher order mode, which depends on the DR and metallic cavity characteristics, is a hybrid mode with one azimuthal variation. If we sum the insertion–loss curves (Fig. 8), taking into account the phases (Fig. 9), we obtain the whole structure response (Fig. 6). Indeed, at the frequency f_3 equal to 5.4 GHz, the S_{21} modulus of each polarization are equal to -10 dB, and the phase difference between these parameters is equal to 180°. Thus, their interference produces a transmission zero. At the frequency f_4, we notice a transmission zero for the two insertion–loss characteristics (Fig. 8). It is due to the interference of each $\mathrm{HEM}_{11\delta}$-mode polarization and the first higher order mode contributions, taking into account the phases. The same analysis applied for the locations $n = 1; 5$ explains the absence of transmission zeros in the filter response.

Finally, as shown in Fig. 6, the response is asymmetrical. In this stage, the objective is to shift f_3 and/or f_4 to produce

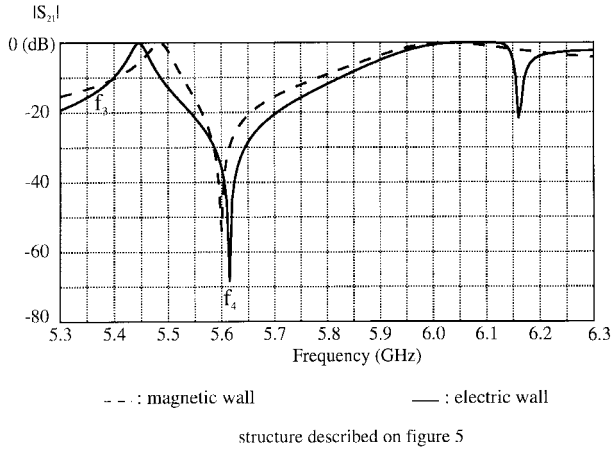

Fig. 8. S_{21} modulus parameter for electric- and magnetic-wall conditions.

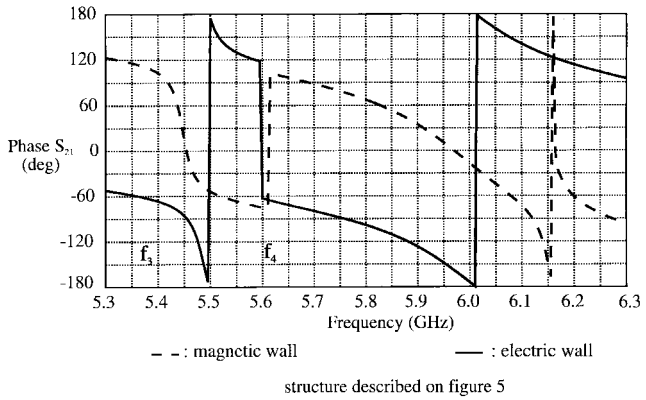

Fig. 9. S_{21} phase parameter for electric- and magnetic-wall conditions.

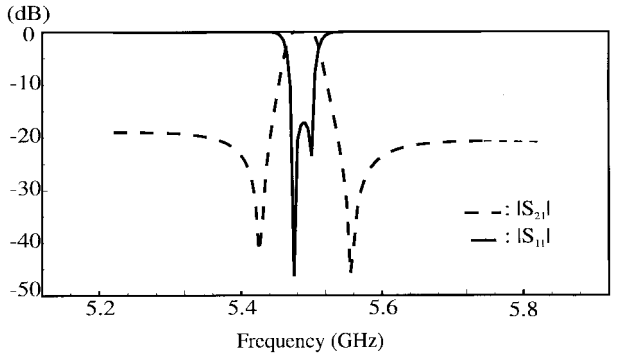

Fig. 10. Symmetrical insertion- and return-loss responses of dual-mode filter.

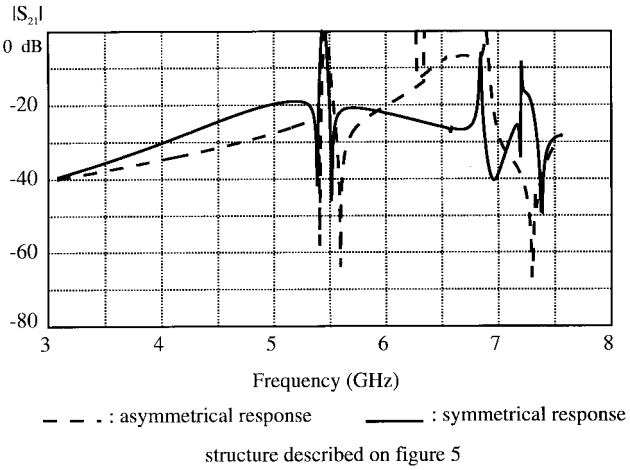

Fig. 11. Out-of-band isolation of asymmetrical and symmetrical dual-mode filter.

a symmetrical dual-mode filter response. The electromagnetic analysis proves that when modifying the metallic cavity dimensions, the first hybrid higher order mode frequency position is not too dependent on the DR $\mathrm{HEM}_{11\delta}$ mode. Thus, if we control the higher order mode position, we control the second transmission zero position as well. From the asymmetrical response, and for a good balance between the external Q_e notch and metallic cavity dimensions, a symmetrical response have been obtained, as shown in Fig. 10. In this case, the metallic cavity diameter has been increased to lower the first hybrid higher order mode resonant frequency. The new diameter is equal to 46 mm. However, the filtering performances can be optimized by any modifications of the DR environment, which modifies the difference between the $\mathrm{HEM}_{11\delta}$ mode and the first hybrid higher order mode resonant frequencies. We show in Fig. 11 that our procedure also permits us to improve the out-of-band isolation presented by the dual-mode filter response.

IV. Dual-Mode DR Filter-Synthesis Method

In this stage, a synthesis method is developed to perform the rigorous design of dual-mode DR filters without tuning. This theoretical method is based on a rigorous analysis of the device using the FEM and on the slotted DR coupling technique.

To realize a microwave filter, the designer must first define some filtering objectives, such as the passband central frequency, bandwidth, insertion losses, and rejection slope. These objectives permit us to define the response shape, number of pole, and coupling matrix which impose the external Q_u factor Q_e and the coupling coefficients between the resonators. Then, to satisfy these electric characteristics, conceivers define a microwave filter topology such as the DR's, shown in Figs. 16 and 21.

These two elliptic dual-mode DR filters with four and eight poles have been chosen to apply our synthesis method. They are composed of a metallic cavity, two input/output coaxial probes, and two or four slotted DR's coupled through a metallic crossing iris.

To compute the dimensions of these devices which will satisfy the electric characteristics given by the filtering objectives, we first develop the segmentation approach presented by the theoretical scheme in Fig. 12.

Applying the free or forced oscillations' 3-D FEM, we compute the following.

1) The DR and metallic cavity dimensions required to obtain the central frequency.
2) The external Q_u factor Q_e linked to the input/output coupling coefficients between a coaxial probe and a classical DR. Q_e depends on the probe penetration depth (Fig. 13). The dimensions of the device described in Fig. 13 are defined by the first step. In this case, only one polarization is excited at the frequency f_0. We consider

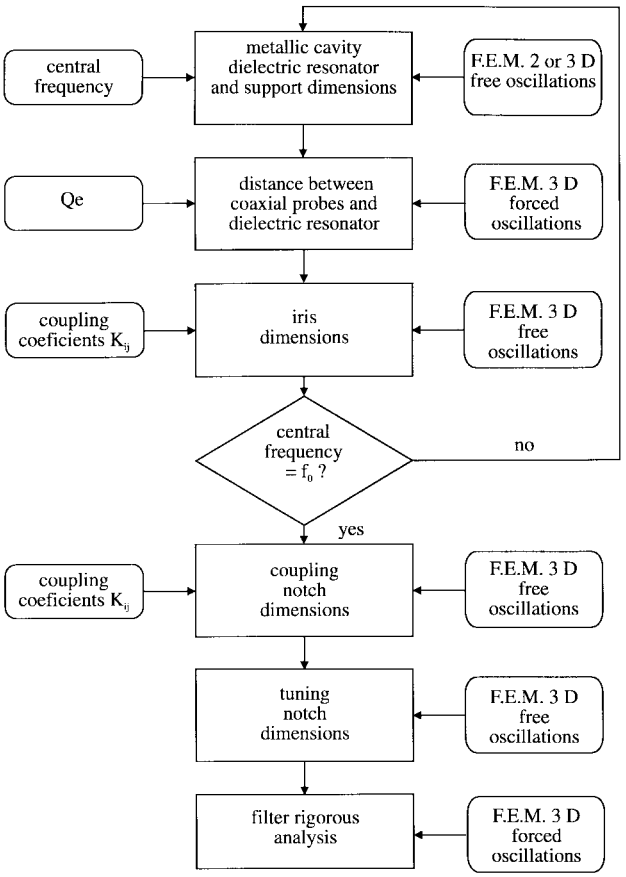

Fig. 12. Rigorous synthesis method.

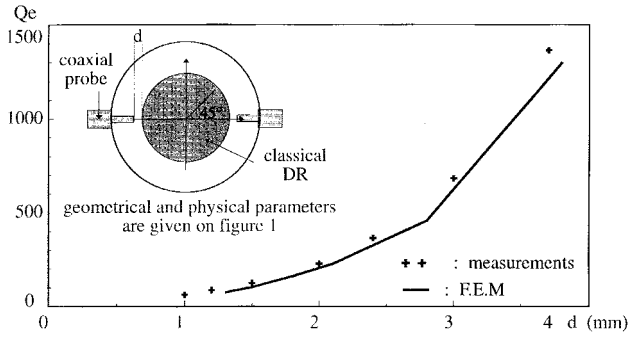

Fig. 13. External Q_u factor.

the bandwidth (Δf) at -3 dB, as the dielectric losses are not taken into account. Thus, we define Q_e with the following equation:

$$Q_e = \frac{f_0}{\Delta f}. \tag{2}$$

3) The coupling coefficients between two classical DR's as a function of a rectangular iris dimensions.

Following the above-mentioned points, the device resonant frequency is known. It can be modified to satisfy the required one, and then we can define: 1) the coupling notch (notch-1) dimensions. With the first step, the metallic cavity and slotted DR dimensions are known. Thus, applying a free-running analysis, the coupling coefficient K is established as a function of the notch-1 dimensions. Then, the K values imposed by the coupling matrix permit us to define the notch-1 dimensions required for the filter realization (see Fig. 14) and 2) the notch-2 dimensions introduced to tune the filter response. This notch must compensate for the influence of the probe on the resonant frequency of the excited polarization. This frequency increases if notch 2 is located at 90° angle with the excitation axis (see Fig. 15), but if notch 2 is located in this axis, the excited frequency is not disturbed. The interface conditions on notch 2 applied to the electromagnetic fields explain those phenomena.

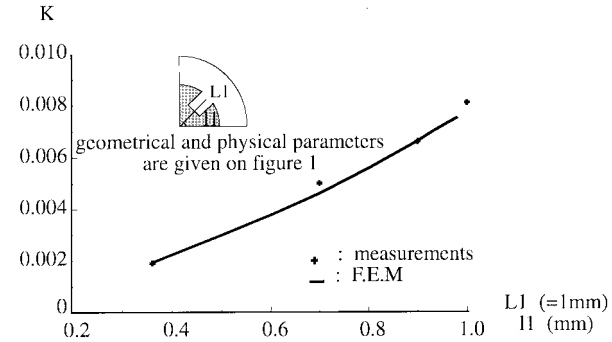

Fig. 14. Coupling coefficient between the two polarizations.

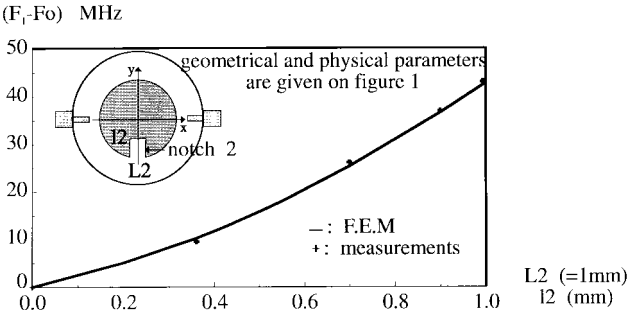

Fig. 15. Frequencies difference between f_0 (classical DR) and f_1 (notch-2 DR).

Then, all the device dimensions are known, but approximately due to the segmentation approach, which does not consider the dependence between the different elements. Thus, in the last step, the scattering parameters are established in the access ports and some coupling iris or notch dimensions must be optimized to satisfy the filtering objectives. During this optimization, filter responses are computed, taking into account slight variations of those dimensions. This procedure is not currently fully automatized.

V. Theoretical and Experimental Results

A four- and an eight-pole elliptic dual-mode slotted-DR filters are now designed using the synthesis method. For these filters, the external Q_e is equal to 108. The central frequency is 5.53 GHz and the bandwidth (-3 dB) is 1%.

A. Four-Pole Elliptic Filter

The filter geometry is given in Fig. 16 and the coupling coefficients matrix is presented in Table I. We notice that notches 1a and 1b are at a 90° angle from each other to obtain a elliptic function.

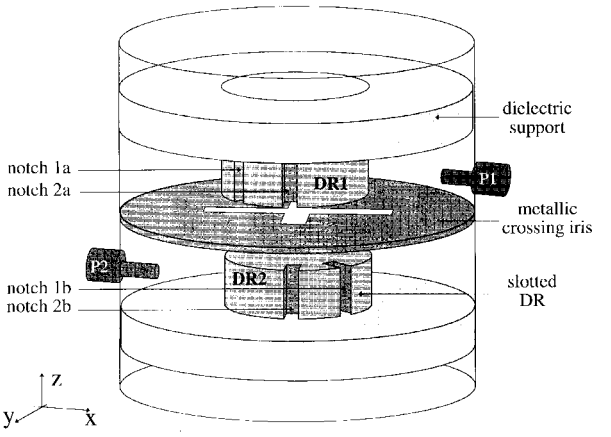

metallic cavity :	dielectric resonator :	crossing iris :
H_C = (14.1 +/- 0.02 *2) mm D_C = 31.0 +/- 0.02 mm	H_{DR} = 3.4 +/- 0.01mm D_{DR} = 15.2 +/- 0.01 mm ε_{DR} = 3 7	(1.00*5.20) +/- 0.02 mm (1.00*7.70) +/- 0.02 mm e = 1.00 +/- 0.01 mm
tuning notches (2a = 2b) :	coupling notches (1a = 1b) :	probe - DR distance :
l2 = 0.62 +/- 0.03 mm L2 = 1.00 +/- 0.03 mm	l1 = 0.93 +/- 0.03 mm L1 = 1.00 +/- 0.03 mm	1.10 +/- 0.01 mm

Fig. 16. Four-pole filter design.

TABLE I
ELLIPTIC FOUR-POLE FILTER: COUPLING-COEFFICIENT MATRIX

Kij	1	2	3	4
1	0	$7.8\ 10^{-3}$	0	0
2	$7.8\ 10^{-3}$	0	$6.55\ 10^{-3}$	$-2.44\ 10^{-3}$
3	0	$6.55\ 10^{-3}$	0	$7.8\ 10^{-3}$
4	$-2.44\ 10^{-3}$	0	$7.8\ 10^{-3}$	0

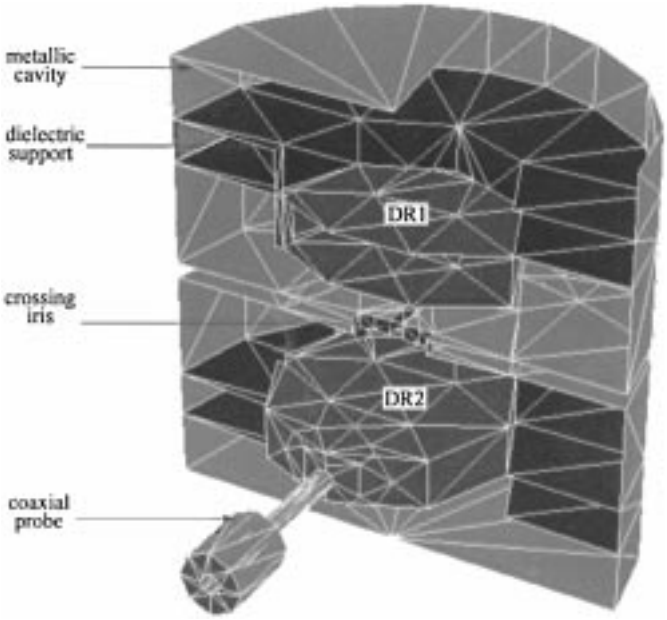

Fig. 17. Four-pole filter mesh.

The mesh of the device is shown in Fig. 17. The four-pole filter theoretical response presented in Fig. 18 is obtained taking into account the dielectric and the metallic losses:

1) for the DR's $\varepsilon_{\mathrm{DR}} = 37 - j37 \cdot tg\delta$ with $tg\delta = f_0\ (\mathrm{GHz})/40\,000$;

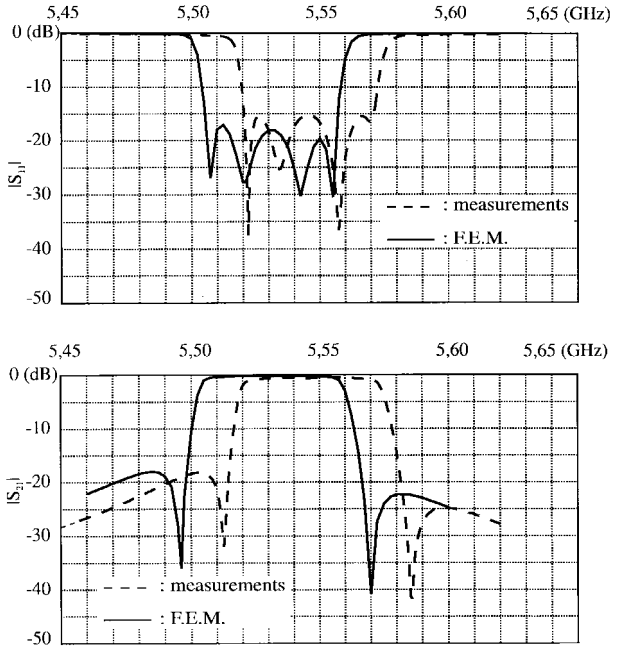

Fig. 18. Four-pole elliptic filter. Computed and experimental return-loss and insertion–loss responses.

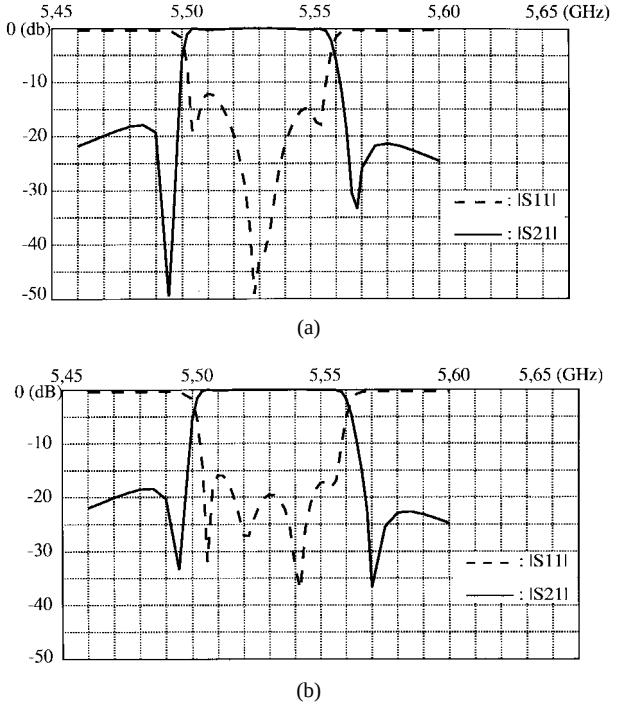

Fig. 19. (a) Four-pole elliptic filter. Sensitivity analysis ($L1 = 1$ mm; $l_1 = 0.93 - 0.01$ mm). (b) Four-pole elliptic filter. Sensitivity analysis ($L_1 = 1$ mm; $l_1 = 0.93 + 0.01$ mm).

2) for the supports $\varepsilon_s = 2.1 - j4.2 \cdot 10^{-4}$;
3) for the metallic walls $\sigma = 1.57 \cdot 10^7$ mho/m.

To describe this filter, we use 9800 nodes and, for the forced running analysis, the computing time is equal to 25 min for one frequency on an HP735 workstation.

An experimental structure without correction on dimensions defined in the last step is built and tested without tuning. Comparisons between theoretical and experimental

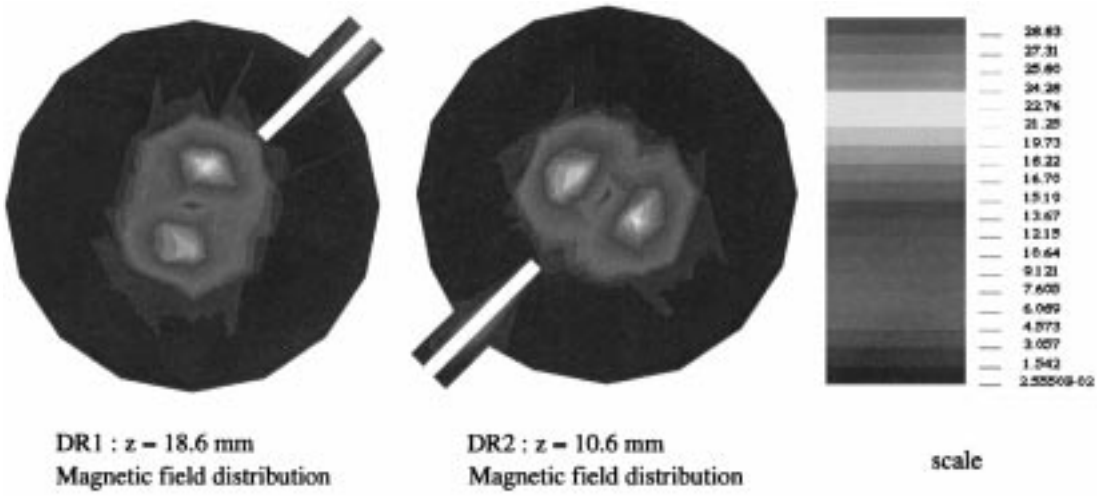

Fig. 20. Electromagnetic-field distributions.

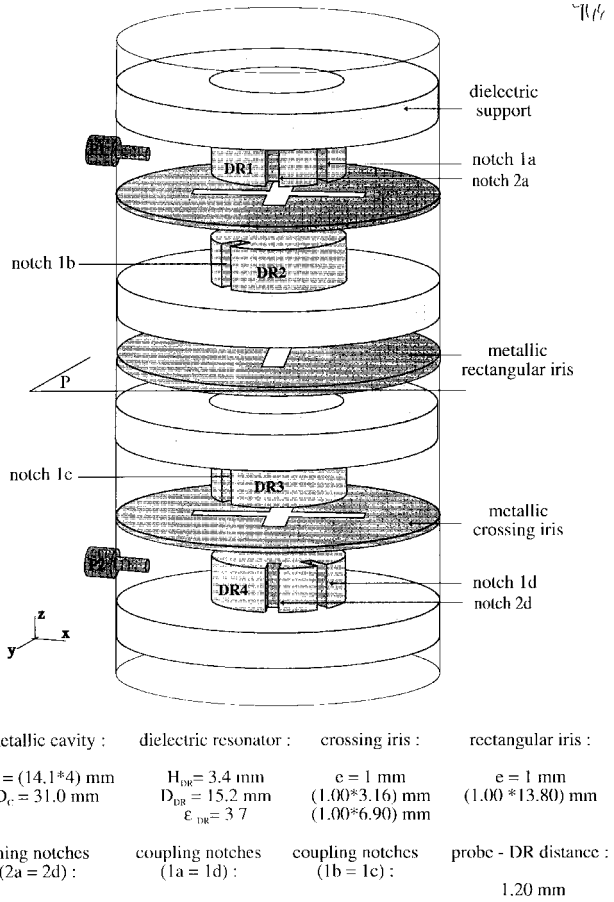

Fig. 21. Eight-pole filter design.

results show encouraging agreement (see Fig. 18). Before the experimental realization, the notches and coupling iris manufacturing tolerances have been defined by applying a sensitivity analysis. For example, curves in Fig. 19(a) and 19(b) prove that the elliptic four-pole filter responses are very sensitive to a diminution equal to 0.01 mm of the coupling notch dimensions. The whole device sensitivity analysis shows that the best filtering performances are obtained for the dimensions and manufacturing tolerances given in Fig. 16. Our software permits us to define the electromagnetic-field distributions during the forced oscillation computations. For example, magnetic-field distributions in DR1 ($z = 18.6$ mm) and in DR2 ($z = 10.6$ mm) are presented in Fig. 20.

TABLE II
ELLIPTIC EIGHT-POLE FILTER: COUPLING-COEFFICIENT MATRIX

Mij	1	2	3	4	5	6	7	8
1	0	$7.5\ 10^{-3}$	0	$-4.7\ 10^{-3}$	0	0	0	0
2	$7.5\ 10^{-3}$	0	$5.6\ 10^{-3}$	0	0	0	0	0
3	0	$5.6\ 10^{-3}$	0	$4.8\ 10^{-3}$	0	0	0	0
4	$-4.7\ 10^{-3}$	0	$4.8\ 10^{-3}$	0	$4.8\ 10^{-3}$	0	0	0
5	0	0	0	$4.8\ 10^{-3}$	0	$4.8\ 10^{-3}$	0	$-4.7\ 10^{-3}$
6	0	0	0	0	$4.8\ 10^{-3}$	0	$5.6\ 10^{-3}$	0
7	0	0	0	0	0	$5.6\ 10^{-3}$	0	$7.5\ 10^{-3}$
8	0	0	0	0	$-4.7\ 10^{-3}$	0	$7.5\ 10^{-3}$	0

B. Eight-Pole Elliptic Filter

The device under consideration is shown in Fig. 21, and the value of the coupling coefficients are presented in Table II.

Our rigorous synthesis method permits us to design the first eight-pole elliptic dual-mode slotted-DR filter. For this device, the permittivities are equal to 37 for the DR's and 2.1 for the supports. To describe the filter with the FEM, we consider one half of the device due to the geometrical symmetries (plane P). Thus, the number of nodes is equal to 9700 and the forced running analysis needs a computing time equal to 40 min for one frequency on an HP735 workstation. The experimental results, obtained without tuning, are presented and compared to the theoretical results in Fig. 22.

C. Conclusion

For the two filters, the difference between the computed central frequency and measured one is less than 0.2%. This shift is attributed to the experimental DR supports, which are slightly different in comparison to the theoretical ones. The difference between the bandwidths is less than 5 MHz, and the experimental passband return loss verifies the theoretical ones.

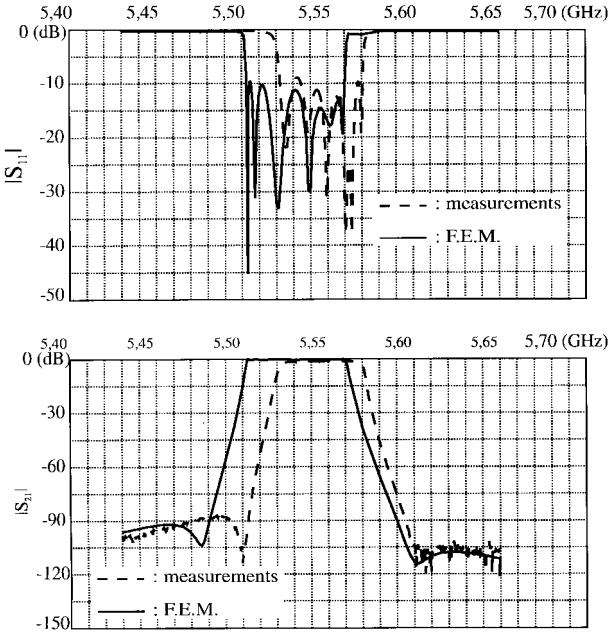

Fig. 22. Eight-pole elliptic filter computed and experimental return-loss and insertion–loss responses.

VI. Conclusion

In this paper, by applying the FEM, complex microwave devices such as dual-mode DR filters are rigorously analyzed.

Firstly, a new dual mode coupling technique is presented which permits us to replace classical DR's, tuning, and coupling screws in the dual-mode DR filter with slotted DR's. Secondly, this paper introduces a new theoretical analysis of dual-mode DR filter responses, based on the interferences between each DR $HEM_{11\delta}$-mode polarization and the higher order modes. This study allows us to define a procedure which explains the presence and controls the position of the two transmission zeros in the filter responses. By using this procedure, we have then obtained a symmetrical dual-mode filter response and better filtering performances. Finally, by applying the FEM, a synthesis method based on the slotted DR coupling technique rigorously designs two elliptic dual-mode DR filters with four and eight poles. During the computations, the DR filter dielectric and metallic losses are taken into account. Before the experimental realizations, some sensitivity analyses have been performed to define some tolerances on the device dimensions.

Thus, for the first time, elliptic dual-mode DR filters with no tuning have been built and tested. The theoretical and experimental elliptic four- and eight-pole filter responses show excellent agreement.

References

[1] X. P. Liang, K. A. Zaki, and A. E. Atia, "Dual mode dielectric or air-filled rectangular waveguide filters" *IEEE Trans. Microwave Theory Tech.*, vol. 42, pp. 1330–1337, July 1994.

[2] J. R. Montejo-Garai and J. Zapata, "Full-wave design and realization of multicoupled dual mode circular waveguide filters" *IEEE Trans. Microwave Theory Tech.*, vol. 43, pp. 1290–1297, June 1995.

[3] M. Guglielmi, "Simple CAD procedure for microwave filters and multiplexers," *IEEE Trans. Microwave Theory Tech.*, vol. 42, pp. 1347–1352, July 1994.

[4] J. A. Curtis and S. J. Fiedziusko, "Multilayered planar filters based on aperture coupled, dual mode microstrip or stripline resonators," in *IEEE MTT-S Dig.*, Albuquerque, NM, June 1–5, 1992, pp. 1203–1206.

[5] R. Doerner, J. Gerdes, C. Rheinfelder, F. J. Schmuckle, W. Heinrich, K. Strohm, F. Schaffler, and J. F. Luy, "Modeling of passive elements for coplanar sige MMIC's" *IEEE MTT-S Dig.*, Albuquerque, NM, June 1–5, 1995, pp. 1187–1190.

[6] A. E. Atia and A. E. Williams, "New types of waveguide bandpass filters satellite transponders" *COMSAT Tech. Rev.*, vol. 1, no. 1, pp. 21–43, Fall 1971.

[7] D. Kajfez, *Dielectric Resonators.* Norwood, MA: Artech House, 1986, ch. 1, pp. 9–62.

[8] D. Baillargeat, S. Verdeyme, P. Guillon, "Elliptic filter rigorous design and modeling applying the finite element method" *IEEE MTT-S Dig.*, Orlando, FL, May 16–20, 1995, pp. 1195–1198.

[9] M. Aubourg and P. Guillon, "A mixed finite formulation of microwave device problems: Application to MIS structure," *J. Electromagn. Waves Applicat.*, vol. 5, no. 415, pp. 371–386, 1991.

[10] V. Madrangeas, S. Verdeyme, M. Aubourg, and P. Guillon, "Modeling microwave boxed structures by 2D and 3D finite element method" *COMPEL*, vol. 13, pp. 337–340, May 1994.

[11] J. C. Nedelec, "A new family of mixed element on R3," *Numer. Math.*, vol. 50, pp. 57–87, 1986.

[12] K. A. Zaki, C. Chen, and A. E. Atia, "A circuit model of probes in dual mode cavities," *IEEE Trans. Microwave Theory Tech.*, vol. 36, pp. 1740–1745, Dec. 1988.

[13] H. L. Thal, Jr., "Microwave filter loss mechanisms and effects" *IEEE Trans. Microwave Theory Tech.*, vol. MTT-30, pp. 1330–1334, Sept. 1982.

[14] M. Guglielmi, "Microstrip ring-resonator dual mode filters" presented at the ESA/ESTEC Workshop: Microwave Filters Space Applicat., Nordwijk, The Netherlands, June 7–8, 1990.

Dominique Baillargeat was born in Le Blanc, France, in December 1967. He received the Doctorat degree from the Université de Limoges, Limoges, France, in 1995.

He is currently Assistant Professor at the Research Institute on Microwave and Optical Communications, University of Limoges, and at the end of 1995, he joined the linear microwave devices team. His research interests concern the development of CAD and optimization tools of microwave devices.

Serge Verdeyme was born in Meihards, France, in June 1963. He received the Doctorat degree from the Université de Limoges, Limoges, France, in 1989.

He is currently Assistant Professor at the Research Institute on Microwave and Optical Communications, Université de Limoges. His main area of interest concern the design and the optimization of microwave devices including DR's.

Michel Aubourg was born in Neuvy Saint-Sépulcre, France, in April 1950. He received the Maitrise of Mathematics, the Doctorate de troisième cycle, and the Doctorat d'Etat degrees from the Université de Limoges, Limoges, France, in 1975, 1978, and1985, respectively.

Since 1979, he has been Chargé de Recherche at the Centre National de Recherche Scientifique (CNRS), France, working at the Microwave Laboratory, Université de Limoge. His main area of interest is application of the FEM in microwave transmission lines.

Pierre Guillon (SM'92) was born in May 1947. He received the Doctorat es Sciences degree from the Université de Limoges, France, in 1978.

From 1971 to 1980, he was with the Microwave and Optical Communications Laboratory, Université de Limoges, where he studied DR's and their applications to microwave and millimeter-wave circuits. From 1981 to 1985, he was a Professor of Electrical Engineering at the University of Poitiers, France. In 1985, he rejoined the Université de Limoges, where he is currently a Professor and Head of the Research Institute on Microwave and Optical Communications, where he works on microwave and millimeter-wave devices.